



Revealing the mechanism of how cardiac myosin-binding protein C N-terminal fragments sensitize thin filaments for myosin binding

Alessio V. Inchingolo^a, Samantha Beck Previs^{b,c}, Michael J. Previs^{b,c}, David M. Warshaw^{b,c,1}, and Neil M. Kad^{a,1}

^aSchool of Biosciences, University of Kent, Canterbury CT2 7NH, United Kingdom; ^bDepartment of Molecular Physiology and Biophysics, University of Vermont, Burlington, VT 05405; and ^cCardiovascular Research Institute, University of Vermont, Burlington, VT 05405

Edited by James A. Spudich, Stanford University School of Medicine, Stanford, CA, and approved February 20, 2019 (received for review September 27, 2018)

Cardiac muscle contraction is triggered by calcium binding to troponin. The consequent movement of tropomyosin permits myosin binding to actin, generating force. Cardiac myosin-binding protein C (cMyBP-C) plays a modulatory role in this activation process. One potential mechanism for the N-terminal domains of cMyBP-C to achieve this is by binding directly to the actin-thin filament at low calcium levels to enhance the movement of tropomyosin. To determine the molecular mechanisms by which cMyBP-C enhances myosin recruitment to the actin-thin filament, we directly visualized fluorescently labeled cMyBP-C N-terminal fragments and GFP-labeled myosin molecules binding to suspended actin-thin filaments in a fluorescence-based single-molecule microscopy assay. Binding of the C0C3 N-terminal cMyBP-C fragment to the thin filament enhanced myosin association at low calcium levels. However, at high calcium levels, C0C3 bound in clusters, blocking myosin binding. Dynamic imaging of thin filament-bound Cy3-C0C3 molecules demonstrated that these fragments diffuse along the thin filament before statically binding, suggesting a mechanism that involves a weak-binding mode to search for access to the thin filament and a tight-binding mode to sensitize the thin filament to calcium, thus enhancing myosin binding. Although shorter N-terminal fragments (Cy3-C0C1 and Cy3-C0C1f) bound to the thin filaments and displayed modes of motion on the thin filament similar to that of the Cy3-C0C3 fragment, the shorter fragments were unable to sensitize the thin filament. Therefore, the longer N-terminal fragment (C0C3) must possess the requisite domains needed to bind specifically to the thin filament in order for the cMyBP-C N terminus to modulate cardiac contractility.

cardiomyopathy | muscle | contractility | single molecule | regulated thin filaments

Cardiac myosin-binding protein C (cMyBP-C) modulates cardiac contraction at the level of the sarcomere. Mutations in the cMyBP-C gene are a major cause of hypertrophic cardiomyopathy (1), a disease that affects up to 1 in 200 people (2) and is the leading cause of sudden cardiac death in young adults (1, 3). cMyBP-C is composed of 11 subdomains from C0 to C10 (Fig. 1A), 8 Ig-like and 3 Fn(III)-like with a proline-alanine-rich region between C0 and C1, and a linker between C1 and C2 (i.e., M-domain) (4). Each cMyBP-C molecule is tethered through its C terminus (5) to the myosin thick filament (6), while its N-terminal domains are free to contact either the myosin head region or the actin thin filament (7) (Fig. 1A). Specifically, cMyBP-C interactions with myosin have been shown to occur through the S2 region (8–11), the myosin regulatory light chain (RLC) (12) and the S1 head (13), which may serve to stabilize myosin's superrelaxed state (14–16) through interactions with the recently defined myosin mesa region (13, 17). In addition to myosin binding, cMyBP-C interacts with actin via its N-terminal domains (C0–C2) (18–21). These binding-partner interactions are believed to functionally impact cardiac contractility. For example, cMyBP-C knockout mouse cardiomyocytes (22) demonstrate a decrease in calcium sensitivity while N-terminal fragments infused into skinned fibers

(11) result in an increase in calcium sensitivity. Accordingly, fluorescence assays in muscle cells (10) have demonstrated that cMyBP-C N-terminal fragments activate muscle at low calcium levels and inhibit maximal activity at high calcium, suggesting dual roles in modulating contraction *in vivo*.

Mechanistically, muscle activation occurs by calcium-dependent shifts in the position of tropomyosin on the thin filament (23, 24). Tropomyosin binds axially along the thin filament (Fig. 1A) and shifts azimuthally when calcium binds to the tropomyosin-associated troponin protein complex. Three positions of tropomyosin have been structurally (24) and functionally (25) defined: blocked (sterically preventing myosin binding), closed (myosin can bind weakly), and open (myosin binding is unperturbed). It has been proposed that the cMyBP-C N terminus could sensitize the thin filament to calcium through the displacement of tropomyosin from its blocked to its closed position, to enhance myosin binding (21). The function of the cMyBP-C N-terminal subdomains C0C3, C0C1, and C0C1f (i.e., C0C1 including the first 17 M-domain residues) have been extensively characterized for their ability to sensitize the thin filament to calcium using *in vitro* motility (18, 26, 27), ATPase assays (19), and electron micrographic studies (18, 21, 28). Our previous studies and that of others show that all three bind to actin, but only the C0C3 fragment can both activate

Significance

Diverse demands on cardiac muscle require the fine-tuning of contraction. Cardiac myosin binding protein-C (cMyBP-C) is involved in this regulation; however, its precise molecular mechanism of action remains uncertain. By imaging the interactions of single myosin and cMyBP-C molecules interacting with suspended thin filaments *in vitro* we observe cMyBP-C N-terminal fragments assist activation and modulate contraction velocity by affecting myosin binding to the thin filament. Fluorescent imaging of Cy3-labeled cMyBP-C revealed that it diffusively scans the thin filament and then strongly binds to displace tropomyosin and activate at low calcium. At high calcium, cMyBP-C decorates the filament more extensively, reducing myosin binding through competing with binding sites. Understanding the mechanism of MyBP-C action has important implications for heart disease.

Author contributions: A.V.I., M.J.P., D.M.W., and N.M.K. designed research; A.V.I., S.B.P., and M.J.P. performed research; A.V.I., M.J.P., D.M.W., and N.M.K. analyzed data; and A.V.I., M.J.P., D.M.W., and N.M.K. wrote the paper.

The authors declare no conflict of interest.

This article is a PNAS Direct Submission.

This open access article is distributed under [Creative Commons Attribution-NonCommercial-NoDerivatives License 4.0 \(CC BY-NC-ND\)](https://creativecommons.org/licenses/by-nc-nd/4.0/).

¹To whom correspondence may be addressed. Email: david.warshaw@uvm.edu or N.Kad@kent.ac.uk.

This article contains supporting information online at www.pnas.org/lookup/suppl/doi:10.1073/pnas.1816480116/-DCSupplemental.

Published online March 15, 2019.

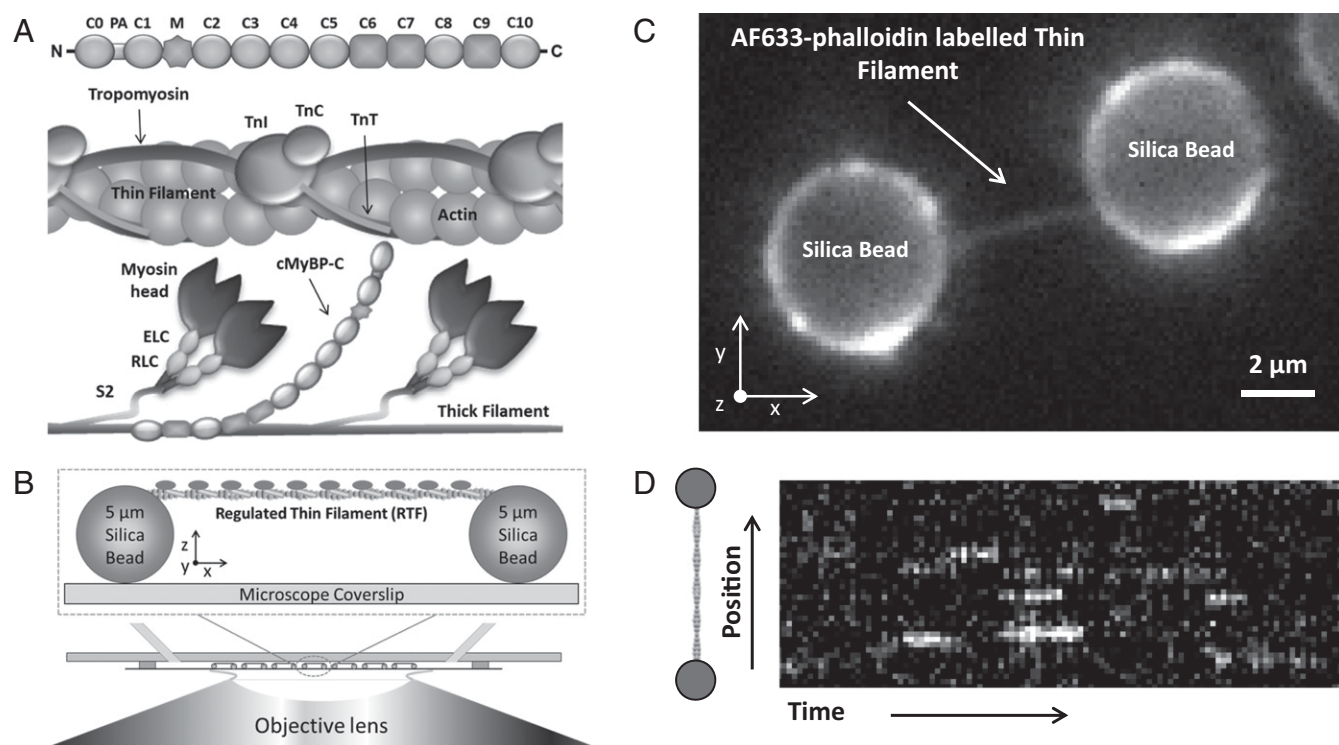


Fig. 1. Thin filaments in vivo and in the single-molecule tightrope assay. (A) The subdomain structure of cMyBP-C and its spatial relationship to the thin filament (actin decorated with tropomyosin and the troponin complex TnI, TnC, and TnT) and myosin-containing thick filament in the sarcomere. (B) The thin-filament tightrope assay. Regulated thin filaments are suspended between surface-adhered beads using a microfluidic device and visualized using a high-N.A. objective lens. (C) A regulated thin filament labeled with AF633-phalloidin can be visualized suspended between two beads. (D) Representative kymograph of interactions between 15 nM S1-GFP and a thin-filament tightrope at high calcium (pCa 4) and 0.1 μM ATP. Each x-axis pixel corresponds to a frame (300 ms), and each pixel on the y axis corresponds to 126.4 nm along the tightrope.

thin filament sliding at low (0.1 μM) calcium and inhibit sliding at high (100 μM) calcium levels. In contrast, the shortest fragment, the murine C0C1, does neither, while the C0C1f with its additional 17 residues of the M-domain can only inhibit thin filament sliding at high calcium (18). These differential functions may allow assignment of specific functional capacities to cMyBP-C's N-terminal domains.

To define the molecular basis of thin-filament activation by cMyBP-C, we used a single-molecule suspended thin filament assay (Fig. 1B), in which we could directly observe the calcium-dependent binding of individual fluorescently labeled myosin-S1 molecules to the thin filament (29). Using all three murine cMyBP-C N-terminal fragments (Fig. 2B), C0C3, C0C1, and C0C1f, we show that cMyBP-C's N terminus (C0C3) can maximally activate the thin filament, permitting myosin-S1 to bind even at low calcium. However, at high calcium with the thin filament maximally activated cMyBP-C can decrease myosin-S1 binding. By imaging fluorescently labeled cMyBP-C N-terminal fragments we observed these molecules individually binding directly to the thin filament. Once bound, the cMyBP-C fragments both diffuse along the thin filament and bind statically, with enhanced static binding observed only for the C0C3 fragment at high calcium levels that maximally activate the thin filament. These fragment binding and motion behaviors on the thin filament provide direct mechanistic insight into how cMyBP-C achieves both calcium sensitization at low calcium and reduced activation at high calcium, and thus modulation of cardiac contractility.

Results

The Effect of cMyBP-C N-Terminal Domains on S1-GFP Myosin Binding to the Thin Filament. We studied how each of the three N-terminal fragments C0C3, C0C1f, and C0C1 (Fig. 2) affects myosin binding

to thin filaments (18–21), by directly measuring individual S1-GFP molecules interacting with thin filaments in their presence. Using 1 μM unlabeled cMyBP-C N-terminal fragments, we determined the level of S1-GFP (15 nM) binding to the thin filament at low and high calcium (0.1 μM and 100 μM , respectively). The fragment concentration was chosen based on past motility studies in which 1 μM C0C3 both sensitized the thin filament to calcium and inhibited thin filament motility at maximally activating calcium concentrations (30). Fig. 2A shows representative kymographs for S1-GFP binding. At low calcium in the absence of C0C3, the kymograph (Fig. 2A, Upper Left) shows very few S1-GFP binding events, consistent with the thin filament's not being fully activated, as previously described (29). At high calcium in the absence of C0C3, the thin filament is activated, as evidenced by significant S1-GFP binding to the thin filament (Fig. 2A, Upper Right). In the presence of C0C3 the situation is reversed. At low calcium, considerable S1-GFP binding is observed (Fig. 2A, Lower Left), whereas at high calcium these interactions are rare (Fig. 2A, Lower Right). To quantify changes in S1-GFP binding, we calculated the mean fluorescence intensity per pixel for each tightrope. Minimally, 10 tightropes were observed under the same experimental condition (Fig. 2B). To compare the effects of a given cMyBP-C fragment on S1-GFP binding, the average fluorescence intensity per pixel was normalized to that at low calcium concentration in the absence of fragments (Fig. 2B). At low calcium, addition of C0C3 significantly increased S1-GFP binding [$57.0 \pm 7.6\%$ (SEM)] vs. no fragment, equivalent to that observed at high calcium in the absence of C0C3 [$55.7 \pm 13.2\%$ (SEM)]. However, addition of C0C3 at high calcium also significantly reduced S1-GFP binding by $38.3 \pm 15.8\%$ (SEM) vs. the absence of C0C3 at high calcium. Interestingly, no significant difference in S1-GFP binding was seen as a result of the introduction of either shorter fragment,

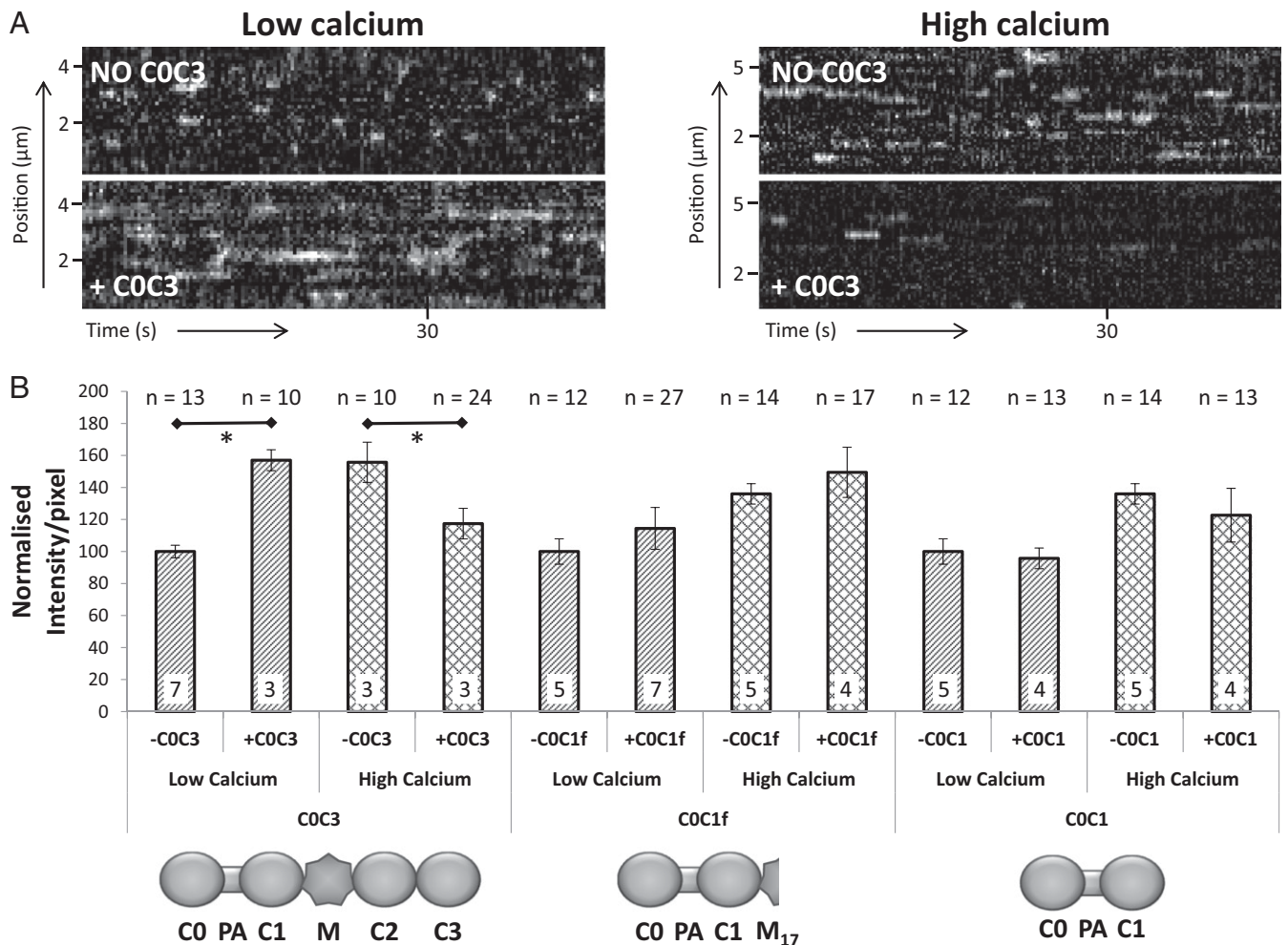


Fig. 2. The calcium-dependent effects of cMyBP-C fragments on S1-GFP binding to regulated thin filaments. (A) Representative kymographs of S1-GFP binding to thin filaments in the absence and presence of COC3, at low and high calcium, collected at 3.3 fps. (B) Bar chart of the average intensity/pixel ratio in the kymographs of S1-GFP binding in the absence and presence of different cMyBP-C N-terminal fragments; the values have been normalized to each respective control experiment (i.e., no fragment present at low $[Ca^{2+}]$). Data were collected using 15 nM S1-GFP with or without 1 μ M of fragment, with n values representing the number of tightropes imaged per condition. The number of experimental repeats (flowcells) is shown at the bottom of the bars. Results showed a significant increase [$57.0 \pm 7.6\%$ (SEM)] in S1-GFP binding in the presence of COC3 at low calcium and reduction [$38.3 \pm 15.8\%$ (SEM)] at high calcium; no significant difference was seen when using the shorter fragment COC1f [$14.4 \pm 15.3\%$ (SEM), $P = 0.42$ at low calcium and $13.4 \pm 16.9\%$ (SEM), $P = 0.42$ at high calcium] and COC1 at low [$-4.3 \pm 10.3\%$ (SEM), $P = 0.70$] and high calcium [$-13.4 \pm 18.0\%$ (SEM), $P = 0.44$]. *Significant at $P < 0.075$.

COC1f or COC1, at both low and high calcium. These results suggest that the shorter fragments are missing critical domains essential for modulating S1-GFP binding to the thin filament in a calcium-dependent manner.

Imaging N-Terminal cMyBP-C Fragments Binding to the Thin Filament.

As described above, only the COC3 fragment affected S1-GFP binding to the thin filament in a calcium-dependent manner. Could the differential effects seen for the COC3 fragment compared with the shorter COC1f and COC1 fragments be related to a difference in their binding to the thin filament? Therefore, we imaged 20 nM Cy3-tagged COC3, COC1f, and COC1 interacting with thin filaments at both low and high calcium. Fig. 3 shows clear binding of all three fragments to the thin filaments using long-exposure (1 s) still images. These images were analyzed to determine the average number of fragment molecules bound per micrometer of thin filament. To ensure a more accurate determination of closely spaced fluorescent fragments that could not be spatially resolved, we used fluorescent spot intensity to estimate the number of molecules per spot. First, we determined the fluorescence intensity for

single Cy3-COC3 molecules from thin filament binding images at low calcium (Fig. 3A, *Left*), where fluorescent spots were easily discernible. Even in these conditions there was considerable variance in spot intensity, suggesting that such spots were due to closely spaced, neighboring Cy3-COC3 molecules. To extract the fluorescent intensity of a single molecule, we fitted the distribution of intensities at low calcium to multiple Gaussians (29, 31) as detailed in *SI Appendix, Fig. S1*. Using the fluorescence intensity of a single Cy3, we converted each fluorescence spot intensity along a tightrope into the number of bound molecules and used this to calculate the average number of cMyBP-C fragments bound per micrometer of thin filament. For Cy3-COC3 (Fig. 3A and D), there was a significant greater than fivefold increase in binding at high vs. low calcium [6.27 ± 1.15 molecules per μ m (SEM, $n = 2$) vs. 0.84 ± 0.17 molecules per μ m (SEM, $n = 11$), respectively]. This was not the case for Cy3-COC1f (Fig. 3B and D), where no significant ($P = 0.55$) change in decoration of thin filaments (in molecules per μ m) was observed between low and high calcium [1.17 ± 0.21 (SEM, $n = 9$) vs. 1.56 ± 0.77 (SEM, $n = 5$) molecules per μ m, respectively]. However, significantly more Cy3-COC1 (Fig. 3C and D)

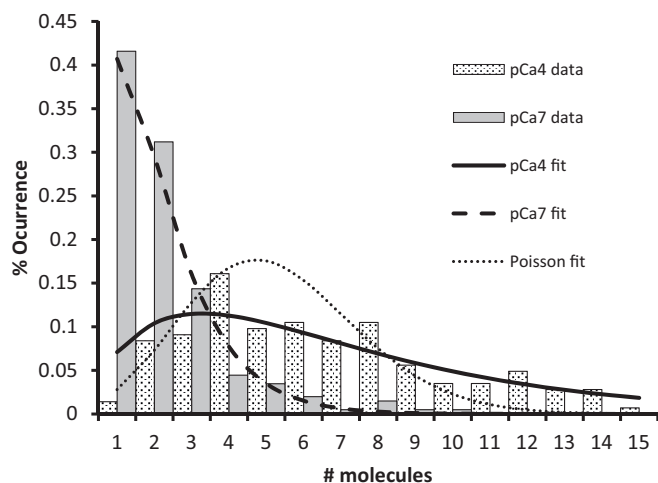


Fig. 4. Histogram of cMyBP-C cluster sizes. The percent occurrence of fluorescent molecules bound to the thin-filament tightropes in clusters was determined based on the fluorescence intensity of a single Cy3-C0C3 (SI Appendix, Fig. S1). Plotted at low calcium (solid bars) and high calcium (dotted bars), data are fitted to the relationship shown in the main text. A best-fit Poisson distribution is shown with the dotted curve. The sum square differences of the Poisson vs. chemical kinetic model are 14.8 and 1.92, respectively, for the high-calcium dataset.

($pA_{Cl}M$; see SI Appendix for mathematical description) and because Cy3-C0C3 binding results in the exposure of more sites on actin, this allows more (i.e., d) Cy3-C0C3 to bind in an effective cooperative unit. Therefore, τ_{off} is expressed as follows:

$$\tau_{off} = 1 / (d \cdot pA_{Cl}M).$$

As in Desai et al. (29), the probability of the exact number (n) of cMyBP-C molecules binding is $prob_{att}^n \times (1 - prob_{att})^{1-n}$, and this equation was used for fitting (Fig. 4).

Fig. 4 shows the fit to the probability of the exact number of Cy3-C0C3 binding performed by the Microsoft Excel GRG Nonlinear fitting engine to globally fit the high and low calcium conditions simultaneously. The affinity (K_{ca}) of calcium binding to thin filaments was fixed at 0.7 μ M (pCa₅₀ of \sim 6.15) based on previous studies (29, 35). Since the size of the cooperative unit is a property of tropomyosin's stiffness, we also fixed the size of the cooperative unit (d) at 11, as previously determined (29). τ_{on} was measured at high calcium as 5.1 (\pm 3.1 >95% CI) s (SI Appendix, Fig. S3). The only fitted parameter K_2 , the affinity of Cy3-C0C3 for the $A_{Cl}M$ state of the thin filament, was found to be 0.18 (\pm 0.02; >95% CI) μ M.

N-Terminal cMyBP-C Fragments Display Two Modes of Motion on Thin Filaments. Dynamic imaging of cMyBP-C fragments on thin filament tightropes unexpectedly revealed that in addition to N-terminal fragments binding statically to thin filaments [Fig. 5A, horizontal trace (arrowhead)] a proportion of the fragments appeared to diffuse randomly along the thin filament [Fig. 5A, trace with y-axis movement (star)]. Statically bound molecules were defined as not showing any apparent movement greater than one pixel in both dimensions (equivalent to 120 nm and 1 s) during the entire detection time window of >200 s [Fig. 5A, horizontal trace (arrowhead)]. This behavior was calcium-dependent for Cy3-C0C3 molecules; the proportion of kymograph traces showing diffusive Cy3-C0C3 motion decreased significantly ($P < 0.075$) from $19.4 \pm 4.6\%$ (SEM, $n = 11$) at low calcium to $6.0 \pm 1.8\%$ (SEM, $n = 8$) at high calcium (Fig. 5B). By comparison, Cy3-C0C1f showed no significant difference ($P = 0.203$) in the proportion of

diffusive molecules at both low and high calcium, $27.3 \pm 2.2\%$ (SEM, $n = 9$) and $32.3 \pm 3.1\%$ (SEM, $n = 6$), respectively. This was also the case for Cy3-C0C1 $24.5 \pm 6.4\%$ (SEM, $n = 7$) vs. $47.7 \pm 26.2\%$ (SEM, $n = 3$) at low and high calcium, respectively ($P = 0.2542$). We also observed that some of the diffusing molecules would switch to static binding during their interaction with the thin filament (SI Appendix, Fig. S4), which was interpreted as being temporarily bound to a specific site in a partially exposed region of the thin filament; nonetheless, these molecules were classified as diffusive.

We calculated the diffusional characteristics summarized in SI Appendix, Table S1 using mean squared displacement (MSD):

$$MSD = \frac{1}{n} \sum_{i=1}^n (x_i(t) - x_i(0))^2 = 2Dt^\alpha,$$

where D is the diffusion constant of the molecule, t is the analysis time window, $x_i(t)$ is the position at time t , $x_i(0)$ is the starting reference position, and α is a coefficient that denotes the nature of the diffusion, where values close to 1 indicate random diffusion (36). Diffusion constants were transformed to log values before averaging and errors propagated to real numbers to provide the values in SI Appendix, Table S1.

Diffusion along a lattice can be described as multiple discrete steps with an average stepping rate. This definition allows us to calculate the average step size of the fragments on the thin filament, provided the stepping rate is known. We can calculate the stepping rate from attached lifetimes obtained from laser trap studies (37) that indicated C0C3, C0C1f, and C0C1 attach with two lifetime populations, <30 ms and >200 ms. Given that the longer events were \sim 60 times less frequently observed, and more likely to represent the a population of the stronger interactions that we report here (SI Appendix, Fig. S3), we used the short lifetime to calculate the step size for each fragment at low calcium, according to the equations below (38):

$$stepping\ rate = \frac{1}{\tau} = \frac{2D}{l^2}$$

$$\therefore step\ size = l = \sqrt{2D\tau},$$

where τ is the attached lifetime, D is the diffusion constant, and l is the average step size. This provides an average step size of 17 ± 3 nm (SD) for Cy3-C0C3, 12 ± 2 nm (SD) for Cy3-C0C1f, and 7 ± 1 nm (SD) for Cy3-C0C1. Due to the method of calculating these values it was not possible to generate a significance test; therefore, these values provide a range of step size from approximately one to three actin monomers.

Discussion

cMyBP-C plays a critical role in modulating cardiac contractility (39, 40), as evidenced by the high prevalence of cMyBP-C mutations in hypertrophic cardiomyopathy (41). One way for cMyBP-C to modulate cardiac contractility is to alter the sensitivity of the thin filament to calcium (10, 18, 27, 39), as reported here. To determine the underlying mechanism by which cMyBP-C enhances thin-filament activation at low calcium levels (18, 26), we directly visualized the impact of cMyBP-C N-terminal fragments on the binding of individual myosin (S1-GFP) molecules along a single suspended actin-thin filament. Specifically, we observed that the C0C3 N-terminal fragment enhanced myosin binding to thin filaments at low calcium (i.e., increased calcium sensitivity) and reduced myosin binding at high calcium. These results are consistent with our previous in vitro motility studies and that of others (18, 26), showing that cMyBP-C's N terminus is sufficient to sensitize the thin filament to calcium and to modulate thin-filament sliding velocities at high calcium. The binding of

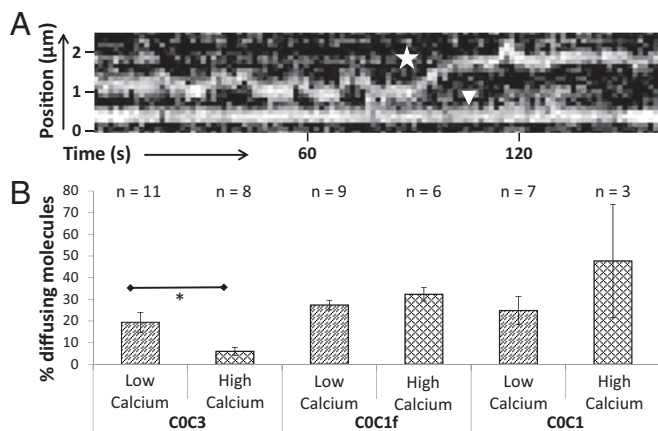


Fig. 5. cMyBP-C fragments diffuse on and statically bind to thin-filament tightropes. (A) An example of a kymograph representing the two types of interaction seen with cMyBP-C (using Cy3-COC3 as an example). Diffusion on the thin-filament tightrope is indicated by a star and a stationary molecule is indicated with an arrowhead. (B) A bar chart providing the mean fraction \pm SEM of diffusing molecules measured at low and high calcium concentrations. n values refer to the number of flowcells. *Significant at $P < 0.075$. Data were collected for 200 s or more using 20 nM of either COC3, COC1f, and COC1 at low calcium; at high calcium, to compensate for decoration levels that enable individual molecules to be distinguished, 5 nM COC3 and COC1f or 20 nM COC1 was used.

Cy3-COC3 itself to the thin filament is seen to occur in clusters and this binding most likely displaces tropomyosin to a position that facilitates myosin binding (10, 18, 20). Surprisingly, $\sim 20\%$ of total Cy3-COC3 binding events show diffusive behavior on the thin filament at low calcium, which may reflect the behavior of cMyBP-C's N terminus within the sarcomere as it searches for its binding site on the thin filament.

Specific cMyBP-C N-Terminal Domains Are Necessary for Thin-Filament Activation. Activation of the thin filament at high calcium triggered significant S1-GFP binding, as expected (Fig. 2). Interestingly, the COC3 N-terminal fragment sensitized the thin filament to calcium so that at low calcium, S1-GFP binding was equivalent to that for a fully calcium-activated thin filament (Fig. 2). The shorter N-terminal fragments (COC1f and COC1), with the C2 and C3 domains and a portion or the entire M-domain removed, were still capable of binding to thin filaments (Fig. 3). However, these fragments failed to sensitize the thin filament at low calcium (Fig. 2), measured as no change in S1-GFP binding in their presence. The failure of these shorter, murine cMyBP-C N-terminal fragments to sensitize the thin filament agrees with ATPase (19), *in vitro* motility (18, 26), and fragment-infused fiber data (11), suggesting that murine N-terminal fragments require at least C0–C2 to observe maximal thin filament calcium sensitization compared with the human N-terminal cMyBP-C fragments, where COC1 and C1 alone are sufficient to sensitize the thin filament to calcium (19, 20, 42, 43). This species difference has been attributed to alternate sequences in the Pro-Ala linker between C0 and C1 as well as C1 itself (44).

The three-state model for thin-filament regulation (25) provides a useful mechanistic context for how COC3 sensitizes the thin filament to calcium. Specifically, calcium binding to the thin filament permits tropomyosin movement on actin to expose myosin binding sites, shifting tropomyosin from the “blocked” to the “closed” position. As a result of myosin binding, tropomyosin is further displaced to the “open” or “myosin” position (24), therefore propagating the binding of additional myosins (29). By COC3 binding to the thin filament at low calcium as it transiently enters the closed position, this N-terminal fragment may stabilize tropomyosin in the closed position, allowing myosin binding to

actin, as supported by structural studies of tropomyosin movement caused by COC2 binding to thin filaments (18). Since our data show a distinct difference between binding at low and high calcium concentrations, this may also suggest that additional binding sites become available once tropomyosin is displaced from the blocked position. The clustered or possible coordinated binding of COC3 most likely represents binding to newly accessible actin adjacent to the location of a previously bound COC3; however, intermolecular interactions between COC3 molecules may also contribute.

Modes of cMyBP-C N-Terminal Interactions with the Thin Filament.

The modular architecture of cMyBP-C provides the potential to structurally compartmentalize its functional capacities. Even though the very N-terminal domains, COC1 and COC1f, bind to actin (20, 21, 45, 46) as we have also shown previously (47), only COC3 possesses the ability to sensitize the thin filament to low calcium while decreasing activation levels at high calcium. Unique to our study is the observation that upon binding of these N-terminal fragments to the thin filament, the fragments either remain stationary or undergo a diffusive-like movement along the thin filament. Specifically, for COC3, how do these two distinct modes of interaction (i.e., 20% diffusing and 80% stationary) contribute to the thin-filament sensitization at low calcium? Multiple sites of N-terminal fragment interactions with the thin filament have been proposed based on actin cross-linking (48), fragment binding to actin in the laser trap (37), and electron microscopy studies (18, 20, 21, 46). At low calcium, tropomyosin on the thin filament should be in a dynamic equilibrium between the blocked and closed states (49). Presumably, the stationary Cy3-COC3 molecules are stereospecifically bound to the thin filament through multiple binding sites, which could effectively shift tropomyosin's equilibrium position to being predominantly closed and thus sensitize the thin filament to calcium. At low calcium the Cy3-COC1 and Cy3-COC1f have the same distribution of diffusing and stationary molecules, and therefore the stationary fractions are not bound in the same manner as Cy3-COC3, given the inability of these shorter fragments to sensitize the thin filament for myosin binding. As individual Ig-domains, both C0 and C1 can bind to the thin filament in several different configurations (20, 42), which is not the case for longer COC2 and COC3 fragments (21, 50). These structural studies support our proposal that the stationary Cy3-COC3 molecules are the result of multiple sites of interaction with the thin filament, necessary to achieve calcium sensitization.

For the 20% of the Cy3-COC3 fragments that diffuse at low calcium, we observed transient switching from diffusion to static binding on thin filaments (SI Appendix, Fig. S4). Such behavior would suggest that the diffusing molecules were interacting with regions of the thin filament more stably. However, for those transient static interactions that did not lead to extended binding this may suggest incomplete formation of a binding interface with the thin filament, which would otherwise result in activation and COC3 recruitment. When diffusing, COC3 molecules must weakly interact with the thin filament with a diffusional step size that we estimate to be between ~ 7 and ~ 17 nm, consistent with one to three actin monomers. This diffusive mode of motion may allow the N terminus of cMyBP-C to maintain contact with and scan the thin filament until such time that specific cMyBP-C binding sites are exposed on actin as tropomyosin undergoes its dynamic equilibrium between blocked and closed positions on the thin filament. Once statically bound to these sites, cMyBP-C may stabilize tropomyosin in the closed position (18, 25). This may also explain why at high calcium where the thin filament is predominantly in the closed state (25), Cy3-COC3 binding to the thin filament is significantly increased (Fig. 3D) and almost entirely stationary (Fig. 5B) as cMyBP-C binding sites on actin would be readily exposed.

The clustering of C0C3 may compete with myosin for actin binding sites, as proposed in structural studies (18, 20, 21, 46) and cosedimentation competition studies (51), explaining the reduction in myosin binding observed on tightropes at high calcium (Fig. 2). Therefore, competitive inhibition of myosin binding by the N terminus of cMyBP-C may be one contributing factor to the reduced thin-filament velocity observed both in the C-zone of native thick filaments (52) and in the motility assay at high calcium (18, 26). However, reduced cross-bridge numbers in limited locations on the thin filament may not be enough to slow motility. It is possible that cMyBP-C binding to the thin filament may provide a load against which the remaining cross-bridges work, in turn slowing velocity (53, 54). Is in vivo clustering of cMyBP-C on the thin filament possible? cMyBP-C is positioned every ~43 nm along the thick filament within the C-zone. Since each thin filament in the muscle lattice is surrounded by three thick filaments, the individual cMyBP-C N termini from these thick filaments could cluster at a common point on the thin filament. In addition, HCM mutations of MyBP-C are known to lead to truncations (55), which could potentially compete with myosin as previously suggested (22). Fluorescence detection of Cy3-C0C3 binding and clustering at low vs. high calcium enabled us to fit the data by a chemical equilibrium model to estimate the affinity of these cMyBP-C fragments for thin filaments as 0.18 μM . This value is ~10-fold tighter than the ~2 μM reported for unregulated actin from ATPase inhibition studies (19) and up to 25-fold tighter than the affinities reported for mouse C0C2 using actin cosedimentation assays (48, 56). Some studies reporting the lower binding affinities (48) used bare actin, whereas thin filaments were used in the present study. Recent findings suggest that tropomyosin may bind cMyBP-C's N terminus (57); therefore, tropomyosin itself could act as a cofactor in the clustered binding of C0C3.

Conclusion

In this paper we addressed the nature of thin-filament activation/inhibition by the N terminus of cMyBP-C. Using a newly developed single-molecule imaging assay, we propose a mechanism by which cMyBP-C interacts with thin filaments using two different binding regimes in relaxing and activating calcium conditions. At low calcium (relaxing conditions), cMyBP-C senses the thin filament for changes in activation state due to positional fluctuations of tropomyosin. Sensing occurs by a weak binding mode in which the N terminus diffuses from actin monomer to monomer. Once specific cMyBP-C binding sites are encountered that allow subdomains C0 through C3 to bind more tightly, cMyBP-C can then effectively shift the tropomyosin equilibrium position from the blocked to the closed state, activating the thin filament. At high calcium (activating conditions), where calcium binding to troponin itself shifts tropomyosin from the blocked to the closed position, cMyBP-C can bind tightly to the thin filament and compete for myosin binding. It is important to note that our studies define the cMyBP-C N-terminal interactions with the thin filament but do not rule out potential interactions with the myosin head region as contributing to the thin filament sensitization. Regardless, our studies provide at least one molecular model for how cMyBP-C carries out its function within the confines of the sarcomere in vivo.

Materials and Methods

Protein Purification. Actin and myosin were purified from chicken pectoralis muscle (58), and recombinant human cardiac tropomyosin and troponin

were expressed in *Escherichia coli* and further purified as described previously (59). Murine cMyBP-C fragments were bacterially expressed with a C-terminal His-tag for purification using a nickel affinity column. Myosin-S1 was produced from whole myosin by papain digestion (60) and labeled with EGFP by exchange of the endogenous RLC with recombinantly expressed EGFP-tagged RLC (29); this construct is termed S1-GFP. Using the proteolytically derived single-headed S1 construct, instead of full-length myosin or heavy meromyosin, simplified interpretation and quantification of the data. Thin filaments were fully reconstituted by incubating actin, tropomyosin, and troponin overnight at 4 °C in 4 mM imidazole, pH 7, 2 mM MgCl_2 , 1 mM DTT, and 0.5 mM ATP (61) with a molar ratio actin: tropomyosin: troponin of 2:0.5:0.25. In all experiments, thin filaments were labeled with AF633-phalloidin (A22284; Invitrogen) for imaging in the flow chamber. For experiments involving cMyBP-C N-terminal fragments binding to thin filaments, the N-terminal fragments (i.e., C0C3, C0C1f, and C0C1; see Fig. 2B) were fluorescently labeled with a maleimide-Cy3 (PA23031; GE Healthcare) as in ref. 62, achieving ~30% labeling efficiency. Based on the C0C3 structure, there is only one surface-exposed reactive cysteine (C248) and thus only one Cy3 dye per labeled N-terminal fragment (62).

The Thin-Filament Tightrope Assay. To nullify any potential surface interference and to permit full, 3D accessibility to all myosin and cMyBP-C binding sites on the thin filament, we suspended thin filaments between surface-adhered beads to create tightropes (Fig. 1B) as described in detail previously (29). Briefly, silica beads were functionalized with 340 $\mu\text{g}/\text{mL}$ poly-L-lysine and adhered to a glass coverslip by infusion into a microfluidic flow cell. To generate tightropes, 500-nM thin filaments were passed across the silica beads multiple times back and forth using a syringe pump. Imaging was performed using a custom-built oblique angle fluorescence microscope (38) that excites the sample with a continuous-wave 20-mW, 488-nm DPSS laser (JDSU) focused off-center at the back-focal plane of a 100 \times objective (1.45 N.A.) to achieve obliquely angled illumination. We detected images (Fig. 1C) through an Optosplit III (Cairn Research) projected onto a Hamamatsu OrcaFlash 4.2 camera.

Data Collection and Analysis. All experiments were performed in either high (100 μM , pCa 4) or low (0.1 μM , pCa 7) calcium buffers of 25 mM imidazole, pH 7.4, 4 mM MgCl_2 , 1 mM EGTA, and KCl adjusted to a final ionic strength of 51 mM using MaxChelator (63). Ten or more tightropes were imaged per condition (details of the conditions are provided in *Results*). Videos of S1-GFP binding to thin filaments were acquired at three frames per second (fps) for up to 1 min, while videos of Cy3-labeled cMyBP-C fragments were acquired at 1 fps for up to 5 min. To determine the spatial and temporal dynamics of S1-GFP or Cy3-labeled cMyBP-C fragments interacting with thin filaments, we transformed movies into kymographs where fluorophore position was plotted along the y axis and time on the x axis (Fig. 1D). Analysis of bound fluorophore position was performed using custom-written macros in ImageJ available online (kadlab.mechanicsanddynamics.com). To measure the extent of S1-GFP binding we integrated the fluorescence intensity over the entire kymograph and normalized to the total number of pixels. All statistical *P* values mentioned were calculated using an unpaired *t* test, and *P* values <0.075 were considered significant. All SEM values were calculated using the number of flowcells, and in the case of comparative calculations SEM is a propagated error and therefore no *n* value is given. For data fitted using Microsoft Excel, the >95% CI values were calculated using the method of Kemmer and Keller (64).

ACKNOWLEDGMENTS. We thank Jeffrey Robbins and James Gulick (Cincinnati Children's Hospital Medical Center) for providing the expressed cMyBP-C N-terminal fragments and Greg Hoepflich, Lynn Chrin, and Christopher Berger (University of Vermont) for fluorescently labeling and characterizing the N-terminal cMyBP-C fragments. This work was supported by National Institutes of Health Grants HL126909 and AR067279 (to D.M.W.) and HL124041 (to M.J.P.) and British Heart Foundation Grant FS/13/69/30504 (to N.M.K. and A.V.I.). This work was also supported in part by a generous gift to D.M.W. from Arnold and Mariel Goran.

1. Maron BJ, Maron MS (2013) Hypertrophic cardiomyopathy. *Lancet* 381:242–255.
2. Semsarian C, Ingles J, Maron MS, Maron BJ (2015) New perspectives on the prevalence of hypertrophic cardiomyopathy. *J Am Coll Cardiol* 65:1249–1254.
3. Harvey PA, Leinwand LA (2011) The cell biology of disease: Cellular mechanisms of cardiomyopathy. *J Cell Biol* 194:355–365.
4. Yasuda M, Koshida S, Sato N, Obinata T (1995) Complete primary structure of chicken cardiac C-protein (MyBP-C) and its expression in developing striated muscles. *J Mol Cell Cardiol* 27:2275–2286.

5. Alyonycheva TN, Mikawa T, Reinach FC, Fischman DA (1997) Isoform-specific interaction of the myosin-binding proteins (MyBPs) with skeletal and cardiac myosin is a property of the C-terminal immunoglobulin domain. *J Biol Chem* 272:20866–20872.
6. Luther PK, et al. (2008) Understanding the organization and role of myosin binding protein C in normal striated muscle by comparison with MyBP-C knockout cardiac muscle. *J Mol Biol* 384:60–72.
7. Luther PK, et al. (2011) Direct visualization of myosin-binding protein C bridging myosin and actin filaments in intact muscle. *Proc Natl Acad Sci USA* 108:11423–11428.

8. Starr R, Offer G (1978) The interaction of C-protein with heavy meromyosin and subfragment-2. *Biochem J* 171:813–816.
9. Gruen M, Gautel M (1999) Mutations in beta-myosin S2 that cause familial hypertrophic cardiomyopathy (FHC) abolish the interaction with the regulatory domain of myosin-binding protein-C. *J Mol Biol* 286:933–949.
10. Kampourakis T, Yan Z, Gautel M, Sun YB, Irving M (2014) Myosin binding protein-C activates thin filaments and inhibits thick filaments in heart muscle cells. *Proc Natl Acad Sci USA* 111:18763–18768.
11. Kunst G, et al. (2000) Myosin binding protein C, a phosphorylation-dependent force regulator in muscle that controls the attachment of myosin heads by its interaction with myosin S2. *Circ Res* 86:51–58.
12. Ratti J, Rostkova E, Gautel M, Pfuhl M (2011) Structure and interactions of myosin-binding protein C domain C0: Cardiac-specific regulation of myosin at its neck? *J Biol Chem* 286:12650–12658.
13. Nag S, et al. (2017) The myosin mesa and the basis of hypercontractility caused by hypertrophic cardiomyopathy mutations. *Nat Struct Mol Biol* 24:525–533.
14. Kensler RW, Craig R, Moss RL (2017) Phosphorylation of cardiac myosin binding protein C releases myosin heads from the surface of cardiac thick filaments. *Proc Natl Acad Sci USA* 114:E1355–E1364.
15. McNamara JW, et al. (2017) MYBPC3 mutations are associated with a reduced super-relaxed state in patients with hypertrophic cardiomyopathy. *PLoS One* 12:e0180064.
16. McNamara JW, et al. (2016) Ablation of cardiac myosin binding protein-C disrupts the super-relaxed state of myosin in murine cardiomyocytes. *J Mol Cell Cardiol* 94:65–71.
17. Trivedi DV, Adhikari AS, Sarkar SS, Ruppel KM, Spudich JA (2018) Hypertrophic cardiomyopathy and the myosin mesa: Viewing an old disease in a new light. *Biophys Rev* 10:27–48.
18. Mun JY, et al. (2014) Myosin-binding protein C displaces tropomyosin to activate cardiac thin filaments and governs their speed by an independent mechanism. *Proc Natl Acad Sci USA* 111:2170–2175.
19. Belknap B, Harris SP, White HD (2014) Modulation of thin filament activation of myosin ATP hydrolysis by N-terminal domains of cardiac myosin binding protein-C. *Biochemistry* 53:6717–6724.
20. Harris SP, Belknap B, Van Sciver RE, White HD, Galkin VE (2016) C0 and C1 N-terminal Ig domains of myosin binding protein C exert different effects on thin filament activation. *Proc Natl Acad Sci USA* 113:1558–1563.
21. Mun JY, et al. (2011) Electron microscopy and 3D reconstruction of F-actin decorated with cardiac myosin-binding protein C (cMyBP-C). *J Mol Biol* 410:214–225.
22. Harris SP, et al. (2002) Hypertrophic cardiomyopathy in cardiac myosin binding protein-C knockout mice. *Circ Res* 90:594–601.
23. Spudich JA, Huxley HE, Finch JT (1972) Regulation of skeletal muscle contraction. II. Structural studies of the interaction of the tropomyosin-troponin complex with actin. *J Mol Biol* 72:619–632.
24. Poole KJ, et al. (2006) A comparison of muscle thin filament models obtained from electron microscopy reconstructions and low-angle X-ray fibre diagrams from non-overlap muscle. *J Struct Biol* 155:273–284.
25. McKillop DF, Geeves MA (1993) Regulation of the interaction between actin and myosin subfragment 1: Evidence for three states of the thin filament. *Biophys J* 65:693–701.
26. Razumova MV, et al. (2006) Effects of the N-terminal domains of myosin binding protein-C in an in vitro motility assay: Evidence for long-lived cross-bridges. *J Biol Chem* 281:35846–35854.
27. Razumova MV, Bezold KL, Tu AY, Regnier M, Harris SP (2008) Contribution of the myosin binding protein C motif to functional effects in permeabilized rat trabeculae. *J Gen Physiol* 132:575–585.
28. Kensler RW, Shaffer JF, Harris SP (2011) Binding of the N-terminal fragment C0-C2 of cardiac MyBP-C to cardiac F-actin. *J Struct Biol* 174:44–51.
29. Desai R, Geeves MA, Kad NM (2015) Using fluorescent myosin to directly visualize cooperative activation of thin filaments. *J Biol Chem* 290:1915–1925.
30. Previs MJ, et al. (2015) Myosin-binding protein C corrects an intrinsic inhomogeneity in cardiac excitation-contraction coupling. *Sci Adv* 1:e1400205.
31. Iino R, Koyama I, Kusumi A (2001) Single molecule imaging of green fluorescent proteins in living cells: E-Cadherin forms oligomers on the free cell surface. *Biophys J* 80:2667–2677.
32. Loong CK, Zhou HX, Chase PB (2012) Persistence length of human cardiac α -tropomyosin measured by single molecule direct probe microscopy. *PLoS One* 7:e39676.
33. Bremel RD, Weber A (1972) Cooperation within actin filament in vertebrate skeletal muscle. *Nat New Biol* 238:97–101.
34. Kad NM, Kim S, Warsaw DM, VanBuren P, Baker JE (2005) Single-myosin crossbridge interactions with actin filaments regulated by troponin-tropomyosin. *Proc Natl Acad Sci USA* 102:16990–16995.
35. Maytum R, Lehrer SS, Geeves MA (1999) Cooperativity and switching within the three-state model of muscle regulation. *Biochemistry* 38:1102–1110.
36. Shlesinger MF, Zaslavsky GM, Klafter J (1993) Strange kinetics. *Nature* 363:31–37.
37. Weith A, et al. (2012) Unique single molecule binding of cardiac myosin binding protein-C to actin and phosphorylation-dependent inhibition of actomyosin motility requires 17 amino acids of the motif domain. *J Mol Cell Cardiol* 52:219–227.
38. Kad NM, Wang H, Kennedy GG, Warsaw DM, Van Houten B (2010) Collaborative dynamic DNA scanning by nucleotide excision repair proteins investigated by single-molecule imaging of quantum-dot-labeled proteins. *Mol Cell* 37:702–713.
39. Previs MJ, Michalek AJ, Warsaw DM (2014) Molecular modulation of actomyosin function by cardiac myosin-binding protein C. *Pflugers Arch* 466:439–444.
40. Sadayappan S, de Tombe PP (2012) Cardiac myosin binding protein-C: Redefining its structure and function. *Biophys Rev* 4:93–106.
41. Marian AJ, Braunwald E (2017) Hypertrophic cardiomyopathy: Genetics, pathogenesis, clinical manifestations, diagnosis, and therapy. *Circ Res* 121:749–770.
42. Risi C, et al. (2018) N-terminal domains of cardiac myosin binding protein C cooperatively activate the thin filament. *Structure* 26:1604–1611.e4.
43. Shaffer JF, Wong P, Bezold KL, Harris SP (2010) Functional differences between the N-terminal domains of mouse and human myosin binding protein-C. *J Biomed Biotechnol* 2010:789798.
44. Shaffer JF, Harris SP (2009) Species-specific differences in the Pro-Ala rich region of cardiac myosin binding protein-C. *J Muscle Res Cell Motil* 30:303–306.
45. Lu Y, Kwan AH, Trehwella J, Jeffries CM (2011) The C0C1 fragment of human cardiac myosin binding protein C has common binding determinants for both actin and myosin. *J Mol Biol* 413:908–913.
46. Orlova A, Galkin VE, Jeffries CM, Egelman EH, Trehwella J (2011) The N-terminal domains of myosin binding protein C can bind polymorphically to F-actin. *J Mol Biol* 412:379–386.
47. Previs MJ, et al. (2016) Phosphorylation and calcium antagonistically tune myosin-binding protein C's structure and function. *Proc Natl Acad Sci USA* 113:3239–3244.
48. Shaffer JF, Kensler RW, Harris SP (2009) The myosin-binding protein C motif binds to F-actin in a phosphorylation-sensitive manner. *J Biol Chem* 284:12318–12327.
49. Schaertl S, Lehrer SS, Geeves MA (1995) Separation and characterization of the two functional regions of troponin involved in muscle thin filament regulation. *Biochemistry* 34:15890–15894.
50. Whitten AE, Jeffries CM, Harris SP, Trehwella J (2008) Cardiac myosin-binding protein C decorates F-actin: Implications for cardiac function. *Proc Natl Acad Sci USA* 105:18360–18365.
51. Saber W, Begin KJ, Warsaw DM, VanBuren P (2008) Cardiac myosin binding protein-C modulates actomyosin binding and kinetics in the in vitro motility assay. *J Mol Cell Cardiol* 44:1053–1061.
52. Previs MJ, Beck Previs S, Gulick J, Robbins J, Warsaw DM (2012) Molecular mechanics of cardiac myosin-binding protein C in native thick filaments. *Science* 337:1215–1218.
53. Walcott S, Docken S, Harris SP (2015) Effects of cardiac myosin binding protein-C on actin motility are explained with a drag-activation-competition model. *Biophys J* 108:10–13.
54. Weith AE, et al. (2012) The extent of cardiac myosin binding protein-C phosphorylation modulates actomyosin function in a graded manner. *J Muscle Res Cell Motil* 33:449–459.
55. Bonne G, Carrier L, Richard P, Hainque B, Schwartz K (1998) Familial hypertrophic cardiomyopathy: From mutations to functional defects. *Circ Res* 83:580–593.
56. Chow ML, Shaffer JF, Harris SP, Dawson JF (2014) Altered interactions between cardiac myosin binding protein-C and α -cardiac actin variants associated with cardiomyopathies. *Arch Biochem Biophys* 550–551:28–32.
57. Witayavanitkul N, et al. (2014) Myocardial infarction-induced N-terminal fragment of cardiac myosin-binding protein C (cMyBP-C) impairs myofilament function in human myocardium. *J Biol Chem* 289:8818–8827.
58. Pardee JD, Spudich JA (1982) Purification of muscle actin. *Methods Enzymol* 85:164–181.
59. Janco M, et al. (2012) α -Tropomyosin with a D175N or E180G mutation in only one chain differs from tropomyosin with mutations in both chains. *Biochemistry* 51:9880–9890.
60. Margossian SS, Lowey S (1982) Preparation of myosin and its subfragments from rabbit skeletal muscle. *Methods Enzymol* 85:55–71.
61. Homsher E, Kim B, Bobkova A, Tobacman LS (1996) Calcium regulation of thin filament movement in an in vitro motility assay. *Biophys J* 70:1881–1892.
62. Colson BA, Thompson AR, Espinoza-Fonseca LM, Thomas DD (2016) Site-directed spectroscopy of cardiac myosin-binding protein C reveals effects of phosphorylation on protein structural dynamics. *Proc Natl Acad Sci USA* 113:3233–3238.
63. Bers DM, Patton CW, Nuccitelli R (2010) A practical guide to the preparation of Ca²⁺ buffers. *Methods in Cell Biology* (Elsevier, Amsterdam), Vol 99, pp 1–26.
64. Kemmer G, Keller S (2010) Nonlinear least-squares data fitting in Excel spreadsheets. *Nat Protoc* 5:267–281.